# Identity-specific coding of future rewards in the human orbitofrontal cortex

Howard, James D ; Gottfried, Jay A ; Tobler, Philippe N ; Kahnt, Thorsten

Abstract: Nervous systems must encode information about the identity of expected outcomes to make adaptive decisions. However, the neural mechanisms underlying identity-specific value signaling remain poorly understood. By manipulating the value and identity of appetizing food odors in a pattern-based imaging paradigm of human classical conditioning, we were able to identify dissociable predictive representations of identity-specific reward in orbitofrontal cortex (OFC) and identity-general reward in ventromedial prefrontal cortex (vmPFC). Reward-related functional coupling between OFC and olfactory (piriform) cortex and between vmPFC and amygdala revealed parallel pathways that support identity-specific and -general predictive signaling. The demonstration of identity-specific value representations in OFC highlights a role for this region in model-based behavior and reveals mechanisms by which appetitive behavior can go awry.

DOI: https://doi.org/10.1073/pnas.1503550112

**SOCIAL SCIENCES: Psychological and Cognitive Sciences**

**BIOLOGICAL SCIENCES: Neuroscience**

# Identity-specific coding of future rewards in the human orbitofrontal cortex

James D. Howard[1], Jay A. Gottfried[1], Philippe N. Tobler[2], Thorsten Kahnt[1]*

[1]*Department of Neurology, Northwestern University Feinberg School of Medicine, Chicago, IL, 60611, United States*

[2]*Department of Economics, University of Zurich, Zurich, 8006, Switzerland*

*__Correspondence__ should be addressed to T.K. (thorsten.kahnt@northwestern.edu)

Northwestern University Feinberg School of Medicine

Department of Neurology

303 E Chicago Ave, Ward 13-006

Chicago IL, 60611, USA

**Keywords:** reward value; multi-voxel pattern analysis; ventromedial prefrontal cortex; associative learning; olfaction

**Abstract**

Nervous systems must encode information about the identity of expected outcomes in order to make adaptive decisions. However, the neural mechanisms underlying identity-specific value signaling remain poorly understood. By manipulating the value and identity of appetizing food odors in a pattern-based imaging paradigm of human classical conditioning, we were able to identify dissociable predictive representations of identity-specific reward in orbitofrontal cortex (OFC) and identity-general reward in ventromedial prefrontal cortex (vmPFC). Reward-related functional coupling between OFC and olfactory (piriform) cortex, and between vmPFC and amygdala, highlighted parallel pathways that support identity-specific and identity-general predictive signaling. The demonstration of identity-specific value representations in OFC highlights a role for this region in model-based behavior, and reveals mechanisms by which appetitive behavior can go awry.

**Significance Statement**

In order to make adaptive choices based on reward-predicting stimuli, organisms must take into account information about both the value and the specific identity of the to-be-obtained reward. Using appetizing food odors and pattern-based fMRI, here we demonstrate that the human orbitofrontal cortex encodes future rewards in the form of identity-specific value codes. That is, even if valued the same, different expected rewards such as pizza and chocolate cake are differently encoded in this region. We further show that identity-specific and identity general value coding regions are functionally linked to distinct regions, and thereby provide a novel account for the neural circuitry that underlies integration of both sensory and affective information to guide reward-related behavior.

Predictive representations of future outcomes are critical for guiding adaptive behavior. In order to choose different types of rewards, such as food, shelter and mates, it is essential that predictive signals contain specific information about the identity of those outcomes. Food rewards differ dramatically in their nutritional composition, and identity-specific cues allow differential foraging depending on current needs of the organism. The absence of precise mappings between predictive reward signals and their intended outcomes would have devastating effects on food-based decisions.

Despite the ecological relevance of outcome-specific predictive codes, most research in human and non-human primates has focused on “common currency” signals of economic values in the orbitofrontal cortex (OFC) (1, 1-3) and ventromedial prefrontal cortex (vmPFC) (4-7). These signals, which by definition are independent of the specific nature of the reward, can be used to compare and choose between alternative outcomes, but are unable to inform expectations about the specific identity of the outcome.. For this, identity-specific representations that conjointly represent information about both affective value (how good is it?) and outcome identity (what is it?) are necessary, and recent data suggest that the OFC is involved in signaling information about specific outcomes (8-13). For instance, many OFC neurons signal both the value and the identity of the predicted outcome (11), and OFC lesions diminish the effects of outcome identity (but not general affective value) on conditioned behavior (12).

Recent imaging work has also begun to address how the human brain encodes predictive information about rewarding outcomes. One study (8) used an fMRI adaptation paradigm to provide evidence for identity-based codes for reward in the OFC. Another investigation (4) used fMRI data from a willingness-to-pay auction in combination with decoding techniques to reveal category-dependent and category-independent value codes in

vmPFC and lateral OFC, respectively. However, neither of these studies varied value independently of identity, and were therefore unable to test for the presence of identity-specific and identity-general value codes in the OFC.

Here we combined an olfactory paradigm of classical conditioning with fMRI pattern-based approaches to test the hypothesis that the human OFC simultaneously encodes both the value and the identity of an expected rewarding outcome. Critically, we took advantage of two unique properties of appetizing food odors to reveal identity-specific value representations. First, food odors act as potent rewards (14-16) whose pleasantness can scale with perceived intensity (17, 18). Second, different food odors vary widely in identity (e.g., chocolate cake vs. pizza) but may still hold similar value. These distinct features enabled us to systematically manipulate outcome value and identity independently within the same stimulus space.

## Results

***Behavior.*** One day before fMRI scanning, hungry subjects ($n$ = 15) (**Fig.1A**) rated the pleasantness of eight food odors, including four sweet odors (cupcake, strawberry, dulce de leche, watermelon) and four savory odors (pizza, sautéed onions, potato chips, barbecue sauce) (**Fig. 1B**). Based on each subject's ratings, we selected one sweet odor and one savory odor that were matched in rated pleasantness. Next, for each subject, low-intensity versions (corresponding to low-value stimuli) and high-intensity versions (corresponding to high-value stimuli) of these two odors were created by adjusting stimulus concentrations via an olfactometer (see **SI Materials and Methods,** and **SI Discussion**). This resulted in a final selection of four odors, comprising a fully balanced two-factorial design (2 identity levels by 2 value levels; **Fig. 1C**). These odors were then

used as unconditioned stimuli (US) in a classical conditioning procedure on the first day of the experiment, wherein each odor was paired with two unique visual conditioned stimuli (CS) (**Fig. 1D**).

Subjects underwent fMRI scanning on the following two days of the study while again receiving the same CS–US pairings (**Fig. 1D**). Pleasantness ratings obtained on both scanning days confirmed the efficacy of our odor intensity manipulation, whereby the two odor identities (sweet and savory) were matched in value for both low and high intensity levels. A two-way repeated-measures ANOVA ($n = 15$) revealed a significant main effect of value ($F_{1,14} = 33.48$, $p < 0.001$), in the absence of a main effect of identity ($F_{1,14} = 0.36$, $p = 0.56$) or value-by-identity interaction ($F_{1,14} = 0.02$, $p = 0.91$; **Fig. 2A**). This profile was also found for CS pleasantness ratings, indicating that the CS images acquired predictive value information about their associated odor outcomes (two-way repeated-measures ANOVA, $n = 15$; main effect of value, $F_{1,14} = 28.86$, $p < 0.001$; main effect of identity, $F_{1,14} = 0.03$, $p = 0.86$; interaction, $F_{1,14} = 0.001$, $p = 0.97$; **Fig. 2B**; see **SI Fig. S1** for individual data). A similar effect was observed in the sniffing responses (sniff amplitude, **Fig. 2C** and **D**), which differed as a function of odor value (two-way repeated-measures ANOVA, $n = 15$; $F_{1,14} = 9.05$, $p = 0.01$), but not identity ($F_{1,14} = 3.60$, $p = 0.08$). Even though there were small but significant differences between low and high value sniffs (% change from low to high: 3.95% and 5.24% for sweet and savory, respectively), there was no significant interaction ($F_{1,14} = 0.14$, $p = 0.71$), indicating that any comparisons between sweet and savory value effects could not be explained by respiratory differences per se. Moreover, all fMRI analyses focused on the CS presentations which were temporarily dissociated from the odor presentations, and for which no differences in respiration were observed (two-way repeated-measures ANOVA, $n = 15$; main effect of value, $F_{1,14} = 0.09$, $p = 0.76$; main effect

of identity, $F_{1,14} = 0.02$, p = 0.89; interaction, $F_{1,14} = 0.47$, p = 0.50). Nevertheless, in order to comprehensively control for any potential breathing-related effects, sniff parameters were included in all fMRI models (19). See **SI Figure S2** for additional analyses on behavioral task performance.

***Identity-specific value codes in OFC.*** The ability to modulate predictive value while "clamping" predictive identity motivated our next efforts to isolate CS-evoked fMRI representations of identity-specific value. We reasoned that if expected value codes contain identity information, then value-related (high vs. low value) patterns of fMRI ensemble activity corresponding to the different outcome identities (sweet vs. savory) should be reliably distinguishable. Using a multivoxel pattern-based searchlight analysis (20), we first computed the value-related multivoxel response patterns during CS presentation (high minus low value), separately for sweet-predictive and savory-predictive CS cues (**Fig. 3A**). In a second step, we used cross-validated support vector machines (SVM) to identify regions in which these value-related response patterns – corresponding to different predicted outcome identities – could be reliably classified (**Fig. 3A**), the idea being that significant decoding accuracy would be observed only if the value-related activity patterns for the two predicted odors are different. We identified robust codes of identity-specific value in three brain areas: lateral OFC (*x*, *y*, *z* coordinates = 42, 36, -16; *t*-test, $n = 15$; $t = 5.72$, $p_{FWE} = 0.022$; **Fig. 3B**), anterior cingulate cortex (ACC; 6, 38, 16; $t = 5.01$, $p_{FWE} = 0.038$; **Fig. 3C**), and hippocampus (38, -16, -16; $t = 4.92$, $p_{FWE} = 0.020$). The cluster in the lateral OFC was located in Brodmann area (BA) 47, roughly corresponding to area 47/12m and 47/12r in the classification of (21), and 47/12m and 47/12o in the classification of (22).

While these findings suggest that the brain encodes predictive values intrinsically linked to specific outcome identities, it is possible that imperfect balancing of relative value (high vs. low) between the sweet and savory odors within individual subjects could have led to spurious decoding. For example, if the sweet-predictive high vs. low reward CS was perceived to be more rewarding than the savory-predictive high vs. low reward CS, then value differences (rather than identity differences alone) could have influenced the observed classification effects. To rule out this potential confound, we tested the correlation between decoding accuracy and a measure of value imbalance, which compares the difference in value between low and high value levels between the two odors (basically, the difference of the differences; see **SI Materials and Methods**). Supporting the notion that decoding was indeed based on identity-specific value patterns, the correlations between value imbalance and decoding accuracy were non-significant in OFC ($r = 0.08$, p = 0.76, **Fig. 3D**), ACC ($r = -0.27$, $P = 0.32$), and hippocampus ($r = -0.12$, $P = 0.66$).

***Identity-general value codes in vmPFC.*** Although we found evidence for identity-specific value codes in the OFC, it remains possible that predictive representations of identity-general value may be encoded elsewhere. We hypothesized that in this instance, value signals would generalize from one odor identity to the other. Thus, by training an SVM on activity patterns from CS images predicting the value of sweet odors (high vs. low value), we should be able to correctly classify activity patterns from CS cues predicting the value of savory odors, and vice versa (**Fig. 4A**). Using this approach, we found significant decoding of general value signals in vmPFC (-8, 38, -10; *t*-test, $n = 15$; $t = 5.19$, $p_{FWE} = 0.03$; **Fig. 4B**). Notably, this relatively small cluster in medial BA 11 (corresponding to area 10m/10r in (21), and 14m in (22)) closely co-localizes with coordinates (x = -7, y = 38, z = -

11) from previous fMRI studies of "common value" (7). To confirm that these findings reflect identity-general value coding, we predicted that greater value mismatch between sweet and savory odors would weaken classification performance. Results show that greater value imbalance between odor identities was correlated with lower decoding accuracy in vmPFC ($r$ = -0.68, p = 0.01; **Fig. 4C**), providing further evidence that this region supports value coding independent of reward identity.

***Independent pathways for identity-specific and general values.*** We next tested whether identity-specific and identity-general predictive value signals are part of a serial network, or whether they reflect independent processes. In the former scenario, general value would be related to identity-specific signals via functional connections between vmPFC and OFC. In the latter scenario, general value would be established independently of identity-specific representations, for example, through links with the amygdala, which is involved in valuation and general affective processing (23, 24) and is strongly connected to vmPFC (25). To test these hypotheses, we used a psychophysical interaction (PPI) model and searched for brain regions in which functional connectivity with vmPFC was modulated by general predictive value (high vs. low), collapsed across the two odor identities. Supporting the concept of an independent pathway, we found significant value-related connectivity changes between vmPFC and amygdala (-27, -4, -17; $t$-test, $n$ = 15; $t$ = 5.77, $p_{FWE}$ = 0.003; **Fig. 5B**), but not OFC ($t$ =- 1.25, $P$ = 0.23). Moreover, we found that subject-specific overall hunger ratings significantly predicted value-related vmPFC-amygdala connectivity ($r$ = 0.58, $P$ = 0.02; **Fig. 5C**), demonstrating that this connection is directly related to the general motivational value of the odors.

The finding that instantiation of general predictive value in vmPFC is not related to identity-specific value information in OFC aligns with observations demonstrating that vmPFC and

OFC reside in largely dissociable anatomical networks (26-28). In turn, we tested whether identity-specific value signals are functionally connected with olfactory cortices where odor identity is represented (29, 30). Using an SVM-based variation of PPI to identify brain regions where value-related OFC connectivity patterns differed between sweet vs. savory predicted odors, we found significant OFC connections with anterior piriform cortex (-27, 14, -20; *t*-test, $n = 15$; $t = 4.08$, $p_{FWE} = 0.014$; **Fig. 5D**) and ACC (-3, 47, 16; $t = 6.20$, $p_{FWE} = 0.011$; **Fig. 5E**), but not vmPFC ($t = 0.87$, $p = 0.40$) or amygdala ($t = 1.83$, $p = 0.10$). These findings imply that identity-specific value signals in OFC are related to odor identity information in piriform cortex, a mechanism in keeping with the known bidirectional projections between these two brain areas (31).

**Discussion**

In order to make adaptive choices, nervous systems must encode information about the identity of expected outcomes. Despite the importance of outcome-specific responding for adaptive and goal-directed behavior, most imaging research has focused on characterizing abstract value representations, while disregarding the specific identity of the reward (with a few expectations; (4, 8)). Here we utilized appetizing food odors as rewards in an fMRI paradigm of human classical conditioning, enabling us to dissociate reward value and identity, and to examine neural representations of identity-specific value using pattern-based fMRI analyses. We found that identity-specific value codes in OFC and identity-general value codes in vmPFC were embedded in parallel functional networks involving primary sensory and limbic regions, respectively.

By applying SVM classifiers to value-related fMRI activity patterns associated with distinct reward identities (i.e., savory and sweet food odors), we found robust identity-specific

value coding in a central/lateral region of the OFC. Although these results are seemingly at odds with the widely held idea that OFC signals a “common currency” for value or affect (2, 3, 7), one cannot claim equivalency in the strength of evidence between the failure to find a distributed general value signal using MVPA, and the finding of single-unit evidence for a common value code in monkey OFC (2). In fact, failure to detect such a code in fMRI does not preclude its existence at the single unit level in either human or monkey OFC.

Nevertheless, our results indicate that predictive representations in the OFC conjointly signal both the identity and the value of the expected outcome in a unified neural code. At the level of single neurons, such a coding scheme could be implemented by units signaling both value and identity, or an interaction between the two. Intriguingly, such neurons have recently been identified in the rat OFC (11), and it is likely that other features of the expected outcome, such as reward location, behavioral responses, and other valueless features are also embedded in these complex predictive codes (2, 32-34). Thus, our findings indicate that predictive outcome representations in the OFC are much more complex than previously thought, and provide critical empirical support for recent proposals suggesting that the OFC plays a fundamental role in model-based behavior by tracking the contents and states of the environment and task structure (35, 36). Interestingly, identity-specific value signals were also identified in ACC and hippocampus. The potential functional relevance of these regions in predictive reward coding is described in the supplemental discussion (see **SI Discussion**).

In contrast to the identity-specific value codes found in OFC, identity-general value codes were found in the vmPFC. Here, patterns of fMRI activity coding for the predicted value of a sweet odor could be used to reliably classify the predicted value of a savory odor, and vice versa. This echoes and extends recent evidence demonstrating that vmPFC activity

patterns generalize across different reward categories (3, 4, 6), such as food items, merchandizing gimmicks, and leisure activities. In these studies, classifiers were trained on exemplars (i.e., different items) associated with different values in one category, and could be used to predict the value of exemplars in another category. In contrast, here we manipulated value while keeping identity constant, and show that value codes generalize across specific identities within a category, thereby providing a rigorous test for identity-independent value codes. However, rather than constituting a ubiquitous feature of the ventral prefrontal cortex, such coding was restricted to a localized portion of vmPFC. This is in line with previous reports (7), and accords with the idea that vmPFC is specialized to perform online evaluations of, and comparisons between, currently expected outcomes (37, 38). Arguably, if vmPFC neurons are indeed able to flexibly code the value of a wide range of stimuli, only a limited number of such neurons would be needed, which may account for why general value representations were confined to a relatively small area of vmPFC.

Strikingly, identity-specific and general value signals revealed in the current study were not serially related to each other, but showed functional connections with a non-overlapping set of brain regions. Whereas general value signals in vmPFC were linked to processing in the amygdala, identity-specific value codes in OFC were related to piriform cortex, and olfactory sensory region corresponding to the sensory modality of the rewards used in the current study. This may highlight a fundamental principle, whereby identity-based sensory features of a reward are extracted from sensory-relevant cortical areas and then further processed in OFC to support the formation of identity-specific value codes. Supporting this model, lateral and posterior areas of OFC have been shown to receive direct projections from a wide range of sensory cortices (26, 39).

The embedding of identity-specific and general value representations in parallel pathways alludes to a functional independence of these two signals. A general value code linked with the amygdala would support comparisons between different rewards (7) and map onto relatively coarse actions such as approach or avoidance behaviors (1, 24). In contrast, an identity-specific pathway tied to sensory cortical representations would support more nuanced and differentiated behaviors (35), and thereby allow that prey is eaten and mates are courted – a differentiation that cannot be made using general value signals alone. Indeed, an inability to generate identity-specific value signals in OFC would have profound consequences for consummatory responses, and lead directly to the types of pathological behaviors, including disinhibition, hyperorality and hypersexuality, that are observed in patients with frontotemporal dementia or with structural damage to limbic brain networks (40, 41). Our findings thus offer unique mechanistic insights and testable predictions that may help target future therapeutic interventions for these disorders.

## Materials and Methods

***Subjects.*** Fifteen healthy subjects (7 male, age 23-29, mean ± SD = 25.53 ± 2.33) with normal or corrected-to-normal vision participated in the study. The study took place at the Northwestern University Feinberg School of Medicine, according to protocols approved by the local Institutional Review Board.

***Experimental design.*** Subjects came into the laboratory on three consecutive days. On the first day, odor stimuli were selected and subjects were trained on the conditioning task. On the second and third days, subjects performed 6 runs of an outcome-prediction task inside the MRI scanner, resulting in a total of 12 runs. On all days, subjects were asked to fast for 6 hours prior to the experiment. According to ratings of hunger provided on a scale

from 1 (not at all hungry) to 10 (very hungry), subjects were sufficiently hungry on each day of testing (day 1 = 8 ± 0.28; day 2 = 7.8 ± 0.28; day 3 = 8 ± 0.22) and had not eaten for approximately 6 hours prior to the experiment (day 1 = 6.4 ± 0.95 h, day 2 = 5.9 ± 0.64 h, day 3 = 6.9 ± 1.03 h). Please refer to **SI Materials and Methods** for details on odor stimulus selection, classical conditioning and outcome prediction task, as well as fMRI data acquisition and pre-processing.

***Odor stimuli and application.*** Pleasant food odors (provided by International Flavors and Fragrances, New York, NY) were used as rewards in the experiment. Specifically, we used four sweet odors (shortcake, strawberry, dulce de leche, and watermelon) and four savory food odors (pizza, sautéed onions, potato chips, and barbecue sauce). For all experimental and rating tasks inside and outside the MRI scanner, odors were delivered directly to the nose of the subject using a custom-built, computer-controlled olfactometer according to previously established methods (19). The olfactometer was equipped with two independent mass flow controllers (Alicat, Tucson, AZ) capable of precisely diluting up to 10 odorants with odorless air, such that we could change odor intensity from trial-to-trial while maintaining perceptual identity.

***Multivoxel pattern analysis for identity-specific value codes.*** To identify identity-specific value codes, we used a searchlight decoding approach (42, 43) that allows information mapping without potentially biasing voxel selection (44), in combination with linear kernel SVM (45). In a first step, we estimated a general linear model (GLM) on the re-aligned functional imaging data from each subject and each scanning run. The purpose of this GLM was to estimate the voxel-wise value-related responses for each of the two odors. Subsequently, these value-related responses were used to search for brain regions that differentially code the value of the two odors. The GLM contained 4 regressors

(duration 1.5 seconds) coding for the onset of the CSs predicting sweet or savory odors, separately for each CS set (regressor 1: CSs from set I predicting high and low sweet; regressor 2: CSs from set I predicting high and low savory; regressor 3: CSs from set II predicting high and low sweet; regressor 4: CSs from set II predicting high and low savory). These four onset regressors were each parametrically modulated by the value of the odor predicted by the CSs (coded as 1 and -1 for high and low value). The GLM also included 4 regressors coding for the onsets of the 4 different odor outcomes (sniffs to low and high sweet odors, and low and high savory odors). All 12 regressors (4 CS onset, 4 CS value, 4 US) were convolved with a canonical hemodynamic response function. The six movement parameters, as well as two regressors accounting for parametric trial-by trial fluctuations in sniff amplitude and sniff duration, were included as nuisance regressors of no interest. The four parametric regressors from this GLM are orthogonalized to the corresponding CS onset regressor, and thus account for value-related variance separately for each odor identity and visual stimulus sets (CS set I sweet, CS set I savory, CS set II sweet, CS set II savory), independent of the variance related to expected odor identity. Thus, the voxel-wise parameter estimates from these parametric regressors represent the value-related responses for the two different odors, as signaled by two different stimulus sets.

In a second step, the parameter estimates from the parametric value regressors were used as input for a SVM decoding analysis to search for identity-specific value representations, while controlling for the visual effects of the CSs. The SVM was performed using the LIBSVM implementation (http://www.csie.ntu.edu.tw/~cjlin/libsvm/) with a linear kernel and a preselected cost parameter of c = 0.01. For each searchlight (all voxels within a radius of 4 voxels surrounding the central voxel (45)), we trained a SVM to

classify value-related responses from sweet vs. savory expected odors as signaled by CSs from set I, and tested the SVM on value-related responses from sweet vs. savory expected odors as signaled by CSs from set II. The procedure was repeated in the opposite direction, by training on the sweet vs. savory value-related responses in CS set II and testing on sweet vs. savory value-related responses in CS set I. Moreover, we also trained on sweet set I vs. savory set II, and tested on sweet set II vs. savory set I, and vice versa (reported results are averaged across all four directions). Importantly, decoding in this analysis can only be above chance if different multivoxel response patterns code the predicted value of the sweet and savory odor identities. Moreover, because we trained and tested the SVM on data from different CS sets, the results of this decoding analysis are independent of the visual features of the predictive CSs.

***Multivoxel pattern analysis for identity-independent value codes.*** To identify identity-independent value codes, we first set up a GLM to estimate response patterns for each unique CS. The GLM contained 8 regressors for the onsets (duration 1.5 seconds) of the 8 different CSs (two sets of CSs predicting low and high sweet, and two sets of CSs predicting low and high savory odors). The GLM also included 4 regressors coding for the onsets of the 4 different odor outcomes and the nuisance regressors (sniff parameters and head motion) described above. The voxel-wise parameter estimates of the first 8 regressors represent the response amplitudes to each of the 8 CSs predicting low and high sweet and savory food odors in each of the 12 scanning runs.

In a second step, these 8 parameter estimates were used as input for a SVM cross-identity decoding analysis to search for identity-independent value representations. For each searchlight, we trained a SVM on response patterns from CSs predicting high vs. low sweet odors, and prediction accuracy was obtained by testing the SVM on response

patterns from CSs predicting high vs. low savory odors. The procedure was repeated in the opposite direction, by training on the predicted value of the savory odors and testing on the predicted value of the sweet odors (reported results are averaged across both directions). All other parameters of the searchlight and the SVM were identical to the decoding analysis for identity-specific values described above. Importantly, this cross-identity decoding accuracy can only be significantly above chance if the same multivoxel response patterns code the predicted value of the sweet and the savory odors. Because sweet and savory odors are predicted by different visual CSs, the results are independent of the visual features of the predictive CSs.

***Psycho-physiological interaction analysis.*** We computed the general value-related functional connectivity of the vmPFC using a psycho-physiological interaction (PPI) analysis as implemented in the gPPI toolbox (46). Specifically, for each subject we estimated a PPI model with CSs predicting high vs. low value as the psychological factor, and seed activation of the vmPFC cluster identified in the identity-independent decoding analysis (defined at $P < 0.001$) as physiological factor. The model also included regressors coding for the onsets of the CSs and USs, as well as the sniff and head motion parameters (described above) as nuisance variables of no interest. Individual contrast images for general value-dependent (high vs. low) connectivity changes with the vmPFC were computed and subjected to voxel-wise group-level analyses.

***Multivoxel psycho-physiological interaction analysis.*** In order to reveal brain regions which show identity-specific value-related connectivity with the OFC, a pattern-based connectivity method is required, because no univariate differences in value-related connectivity were expected between the two predicted odor identities (because of the distributed nature of odor coding (29, 30)). Accordingly, we combined the PPI analysis with

the multivoxel pattern analysis described above (see *Multivoxel pattern analysis for identity-specific value codes*). In a first step, for each scanning run, we estimated a PPI model for value-related connectivity as described above (see *Psycho-physiological interaction analysis*) using the OFC (cluster defined at $p < 0.001$ from the identity-specific decoding analysis) as a seed region. In this model, however, we computed the value-related connectivity estimated separately for CSs predicting sweet and savory odors. In a second step, we used these identity-specific value-related connectivity estimates as input to a leave-one-run-out cross-validated SVM searchlight analysis in order to identify brain regions that show different value-related connectivity patterns with the OFC for sweet vs. savory predicted odors. Specifically, instead of using the value-related response amplitudes for different predicted odors to train the SVM (as used in the identity-specific decoding analysis described above), here we used the voxel-wise sweet and savory value-related OFC connectivity estimates to search for brain regions where predicted odor identity could be decoded.

***Group-level analysis.*** To test for significant general and identity-specific value coding, we performed group-level analyses ($n = 15$ subjects) by using voxel-wise one-sample *t*-tests on smoothed accuracy maps (6 mm FWHM). All group-level analyses were carried out in an explicit anatomical mask comprising the orbitofrontal cortex, anterior cingulate cortex, insula, anterior and posterior piriform cortex, amygdala, and hippocampus. To control for relative value differences between odor identities across subjects, all group-level analyses included a measure of value imbalance (defined above) for CS and US ratings as covariates of no interest. The same tests were used to identify regions showing functional connectivity with the vmPFC and OFC. We applied a statistical threshold of $P < 0.05$, corrected for multiple comparisons (familywise error rate, FWE). Based on a priori

hypotheses regarding encoding of identity-independent and identity-specific value, correction was performed for the following anatomical regions of interest from the automated anatomical labeling (AAL) atlas: OFC (superior orbital gyrus, middle orbital gyrus and inferior orbital gyrus), vmPFC (gyrus rectus, medial orbital gyrus), ACC (anterior cingulate cortex), anterior piriform cortex, amygdala, and hippocampus. For display purposes, all imaging results are presented at $p < 0.001$ uncorrected.

**Acknowledgments.** This work was supported by National Institute on Deafness and Other Communication Disorders (NIDCD) grants 1F31DC013500 (J.D.H) and R01DC010014 (J.A.G), and the Swiss National Science Foundation PP00P1_128574, PP00P1_150739, and CRSII3_141965 (P.N.T). Special thanks to International Flavors and Fragrances (S. Miller and S. Warrenburg) for providing yummy food odorants and Sydni Cole for assistance in acquiring the fMRI data.

References


1. Morrison SE, Salzman CD (2009) The convergence of information about rewarding and aversive stimuli in single neurons. *J Neurosci* 29:11471-11483.

2. Padoa-Schioppa C, Assad JA (2006) Neurons in the orbitofrontal cortex encode economic value. *Nature* 441:223-226.

3. Chikazoe J, Lee DH, Kriegeskorte N, Anderson AK (2014) Population coding of affect across stimuli, modalities and individuals. *Nat Neurosci* 17:1114-1122.

4. McNamee D, Rangel A, O'Doherty JP (2013) Category-dependent and category-independent goal-value codes in human ventromedial prefrontal cortex. *Nat Neurosci* 16:479-485.

5. Kable JW, Glimcher PW (2009) The neurobiology of decision: consensus and controversy. *Neuron* 63:733-745.

6. Gross J et al. (2014) Value signals in the prefrontal cortex predict individual preferences across reward categories. *J Neurosci* 34:7580-7586.

7. Levy DJ, Glimcher PW (2012) The root of all value: a neural common currency for choice. *Curr Opin Neurobiol* 22:1027-1038.

8. Klein-Flugge MC et al. (2013) Segregated Encoding of Reward-Identity and Stimulus-Reward Associations in Human Orbitofrontal Cortex. *J Neurosci* 33:3202-3211.

9. Rudebeck PH, Murray EA (2014) The Orbitofrontal Oracle: Cortical Mechanisms for the Prediction and Evaluation of Specific Behavioral Outcomes. *Neuron* 84:1143-1156.

10. Sescousse G, Redoute J, Dreher JC (2010) The architecture of reward value coding in the human orbitofrontal cortex. *J Neurosci* 30:13095-13104.

11. Stalnaker TA et al. (2014) Orbitofrontal neurons infer the value and identity of predicted outcomes. *Nat Commun* 5:3926.

12. Burke KA, Franz TM, Miller DN, Schoenbaum G (2008) The role of the orbitofrontal cortex in the pursuit of happiness and more specific rewards. *Nature* 454:340-344.

13. McDannald MA et al. (2014) Orbitofrontal neurons acquire responses to 'valueless' Pavlovian cues during unblocking. *Elife (Cambridge)*e02653.

14. Gottfried JA, O'Doherty J, Dolan RJ (2003) Encoding predictive reward value in human amygdala and orbitofrontal cortex. *Science* 301:1104-1107.

15. Small DM et al. (2008) Separable substrates for anticipatory and consummatory food chemosensation. *Neuron* 57:786-797.

16. O'Doherty JP et al. (2000) Sensory-specific satiety-related olfactory activation of the human orbitofrontal cortex. *Neuroreport* 11:893-897.

17. Moskowitz HR, Dravnieks A, Klarman LA (1976) Odor Intensity and Pleasantness for A Diverse Set of Odorants. *Perception & Psychophysics* 19:122-128.

18. Gottfried JA, Dolan RJ (2004) Human orbitofrontal cortex mediates extinction learning while accessing conditioned representations of value. *Nat Neurosci* 7:1144-1152.

19. Gottfried JA, Deichmann R, Winston JS, Dolan RJ (2002) Functional heterogeneity in human olfactory cortex: an event-related functional magnetic resonance imaging study. *J Neurosci* 22:10819-10828.

20. Kahnt T, Park SQ, Haynes JD, Tobler PN (2014) Disentangling neural representations of value and salience in the human brain. *Proc Natl Acad Sci U S A* 111:5000-5005.

21. Ongur D, Ferry AT, Price JL (2003) Architectonic subdivision of the human orbital and medial prefrontal cortex. *J Comp Neurol* 460:425-449.

22. Mackey S, Petrides M (2010) Quantitative demonstration of comparable architectonic areas within the ventromedial and lateral orbital frontal cortex in the human and the macaque monkey brains. *Eur J Neurosci* 32:1940-1950.

23. Baxter MG, Murray EA (2002) The amygdala and reward. *Nat Rev Neurosci* 3:563-573.

24. Paton JJ, Belova MA, Morrison SE, Salzman CD (2006) The primate amygdala represents the positive and negative value of visual stimuli during learning. *Nature* 439:865-870.

25. Amaral DG, Prince JL (1984) Amygdalo-cortical projections in the monkey (Macaca fascicularis). *J Comp Neurol* 230:465-496.

26. Carmichael ST, Price JL (1996) Connectional networks within the orbital and medial prefrontal cortex of macaque monkeys. *J Comp Neurol* 371:179-207.

27. Zald DH et al. (2014) Meta-analytic connectivity modeling reveals differential functional connectivity of the medial and lateral orbitofrontal cortex. *Cereb Cortex* 24:232-248.

28. Kahnt T et al. (2012) Connectivity-Based Parcellation of the Human Orbitofrontal Cortex. *J Neurosci* 32:6240-6250.

29. Howard JD et al. (2009) Odor quality coding and categorization in human posterior piriform cortex. *Nat Neurosci* 12:932-938.

30. Zelano C, Mohanty A, Gottfried JA (2011) Olfactory predictive codes and stimulus templates in piriform cortex. *Neuron* 72:178-187.

31. Carmichael ST, Clugnet MC, Price JL (1994) Central olfactory connections in the macaque monkey. *J Comp Neurol* 346:403-434.

32. Furuyashiki T, Holland PC, Gallagher M (2008) Rat orbitofrontal cortex separately encodes response and outcome information during performance of goal-directed behavior. *J Neurosci* 28:5127-5138.

33. Feierstein CE et al. (2006) Representation of spatial goals in rat orbitofrontal cortex. *Neuron* 51:495-507.

34. Kennerley SW, Behrens TE, Wallis JD (2011) Double dissociation of value computations in orbitofrontal and anterior cingulate neurons. *Nat Neurosci* 14:1581-1589.

35. Jones JL et al. (2012) Orbitofrontal cortex supports behavior and learning using inferred but not cached values. *Science* 338:953-956.

36. Wilson RC, Takahashi YK, Schoenbaum G, Niv Y (2014) Orbitofrontal cortex as a cognitive map of task space. *Neuron* 81:267-279.

37. Strait CE, Blanchard TC, Hayden BY (2014) Reward value comparison via mutual inhibition in ventromedial prefrontal cortex. *Neuron* 82:1357-1366.

38. Barron HC, Dolan RJ, Behrens TE (2013) Online evaluation of novel choices by simultaneous representation of multiple memories. *Nat Neurosci* 16:1492-1498.

39. Cavada C et al. (2000) The anatomical connections of the macaque monkey orbitofrontal cortex. A review. *Cereb Cortex* 10:220-242.

40. Woolley JD et al. (2007) Binge eating is associated with right orbitofrontal-insular-striatal atrophy in frontotemporal dementia. *Neurology* 69:1424-1433.

41. Miller BL et al. (1986) Hypersexuality or altered sexual preference following brain injury. *J Neurol Neurosurg Psychiatry* 49:867-873.

42. Kriegeskorte N, Goebel R, Bandettini P (2006) Information-based functional brain mapping. *Proc Natl Acad Sci U S A* 103:3863-3868.

43. Haynes JD et al. (2007) Reading hidden intentions in the human brain. *Curr Biol* 17:323-328.

44. Kriegeskorte N, Simmons WK, Bellgowan PS, Baker CI (2009) Circular analysis in systems neuroscience: the dangers of double dipping. *Nat Neurosci* 12:535-540.

45. Kahnt T, Heinzle J, Park SQ, Haynes JD (2010) The neural code of reward anticipation in human orbitofrontal cortex. *Proc Natl Acad Sci U S A* 107:6010-6015.

46. McLaren DG, Ries ML, Xu G, Johnson SC (2012) A generalized form of context-dependent psychophysiological interactions (gPPI): A comparison to standard approaches. *Neuroimage* 61:1277-1286.

47. Lim J, Wood A, Green BG (2009) Derivation and Evaluation of a Labeled Hedonic Scale. *Chem Senses* 34:739-751.

48. McDannald MA et al. (2011) Ventral striatum and orbitofrontal cortex are both required for model-based, but not model-free, reinforcement learning. *J Neurosci* 31:2700-2705.

49. Wu KN et al. (2012) Olfactory input is critical for sustaining odor quality codes in human orbitofrontal cortex. *Nat Neurosci* 15:1313-1319.

50. Platt ML, Glimcher PW (1999) Neural correlates of decision variables in parietal cortex. *Nature* 400:233-238.

51. Chang SW, Gariepy JF, Platt ML (2013) Neuronal reference frames for social decisions in primate frontal cortex. *Nat Neurosci* 16:243-250.

52. Hollon NG et al. (2014) Dopamine-associated cached values are not sufficient as the basis for action selection. *Proc Natl Acad Sci U S A* 111:18357-18362.

53. Roesch MR, Olson CR (2004) Neuronal activity related to reward value and motivation in primate frontal cortex. *Science* 304:307-310.

54. Leathers ML, Olson CR (2012) In monkeys making value-based decisions, LIP neurons encode cue salience and not action value. *Science* 338:132-135.

55. Bromberg-Martin ES, Hikosaka O (2011) Lateral habenula neurons signal errors in the prediction of reward information. *Nat Neurosci* 14:1209-1216.

56. Bromberg-Martin ES, Hikosaka O (2009) Midbrain dopamine neurons signal preference for advance information about upcoming rewards. *Neuron* 63:119-126.

57. Tobler PN, Fiorillo CD, Schultz W (2005) Adaptive coding of reward value by dopamine neurons. *Science* 307:1642-1645.

58. van Duuren E, Lankelma J, Pennartz CM (2008) Population coding of reward magnitude in the orbitofrontal cortex of the rat. *J Neurosci* 28:8590-8603.

59. Anderson AK et al. (2003) Dissociated neural representations of intensity and valence in human olfaction. *Nat Neurosci* 6:196-202.

60. Rolls ET, Kringelbach ML, de A, I (2003) Different representations of pleasant and unpleasant odours in the human brain. *Eur J Neurosci* 18:695-703.

61. Howard JD, Gottfried JA (2014) Configural and elemental coding of natural odor mixture components in the human brain. *Neuron* 84:857-869.

62. Luk CH, Wallis JD (2013) Choice Coding in Frontal Cortex during Stimulus-Guided or Action-Guided Decision-Making. *J Neurosci* 33:1864-1871.

63. Rushworth MF et al. (2011) Frontal cortex and reward-guided learning and decision-making. *Neuron* 70:1054-1069.

64. Kolling N, Behrens TE, Mars RB, Rushworth MF (2012) Neural mechanisms of foraging. *Science* 336:95-98.

65. Hayden BY, Pearson JM, Platt ML (2011) Neuronal basis of sequential foraging decisions in a patchy environment. *Nat Neurosci* 14:933-939.

66. Shenhav A, Straccia MA, Cohen JD, Botvinick MM (2014) Anterior cingulate engagement in a foraging context reflects choice difficulty, not foraging value. *Nat Neurosci* 17:1249-1254.

67. Hayden BY, Heilbronner SR, Pearson JM, Platt ML (2011) Surprise signals in anterior cingulate cortex: neuronal encoding of unsigned reward prediction errors driving adjustment in behavior. *J Neurosci* 31:4178-4187.

68. Alexander WH, Brown JW (2011) Medial prefrontal cortex as an action-outcome predictor. *Nat Neurosci* 14:1338-1344.

69. Wimmer GE, Shohamy D (2012) Preference by association: how memory mechanisms in the hippocampus bias decisions. *Science* 338:270-273.

70. Shohamy D, Wagner AD (2008) Integrating memories in the human brain: hippocampal-midbrain encoding of overlapping events. *Neuron* 60:378-389.

71. Wimmer GE, Daw ND, Shohamy D (2012) Generalization of value in reinforcement learning by humans. *Eur J Neurosci* 35:1092-1104.

72. Kahnt T, Park SQ, Burke CJ, Tobler PN (2012) How glitter relates to gold: Similarity-dependent reward prediction errors in the human striatum. *J Neurosci* 32:16521-16529.

## Figure Legends

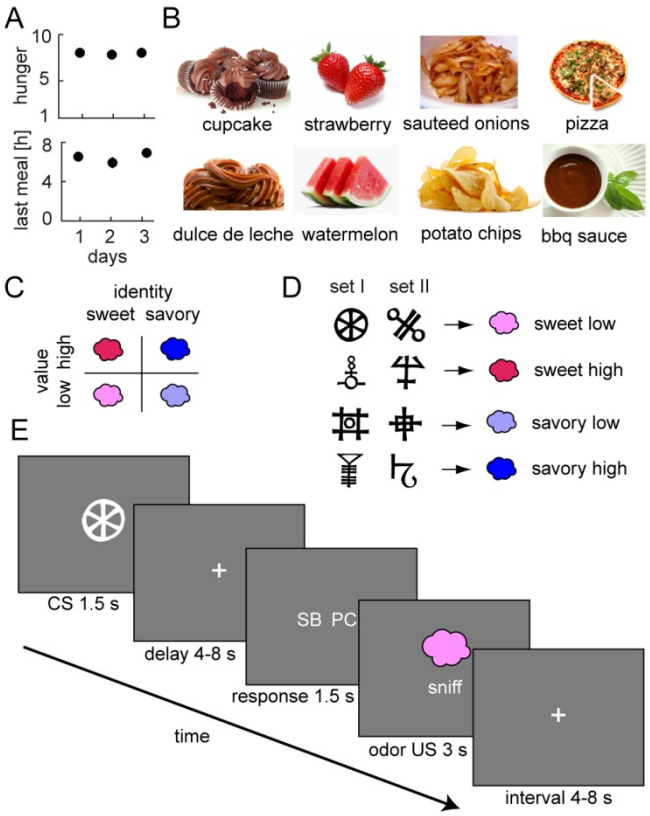


**Figure 1.** Experimental design and stimuli. (**A**) Hunger ratings (top) and time-to-last-meal (bottom) did not differ across days (one-way ANOVAs: hunger, $F_{2, 28} = 0.34$, p = 0.71; time-to-last-meal, $F_{2,28} = 0.97$, p = 0.39). Note, error bars for SEM. ($n = 15$) are smaller than the symbols. (**B**) Pictorial representations of the sweet and savory food odor stimuli used in the experiment. (**C**) Illustration of the two-factorial design of our study, in which value (low vs. high) and identity (sweet vs. savory) could be independently manipulated. (**D**) Subjects learned to associate each of the four odor US with two unique visual CS, resulting in two stimulus sets. (**E**) On each trial of the fMRI task, one of the eight CS images was presented, and subjects had to predict either the value of the upcoming US (response options: low [“L”] and high [“H”]) or the identity of the upcoming US (response options, in

this example: strawberry [“SB”] and potato chips [“PC”]). This prediction was followed by a sniff cue and delivery of odor.

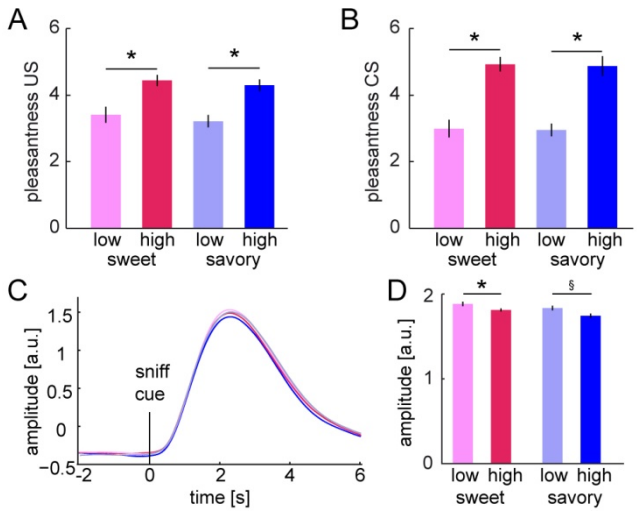


**Figure 2.** Pleasantness ratings and breathing data. (**A-B**) Pleasantness ratings of the US (**A**) and the CS (**B**) were systematically higher for high vs. low intensity stimuli (paired *t*-tests). (**C**) Average sniff responses locked to the sniff cue. (**D**) Average peak sniff amplitudes. *t*-test ($n = 15$), * $p < 0.05$, § $p = 0.052$. Error bars, SEM. ($n = 15$).

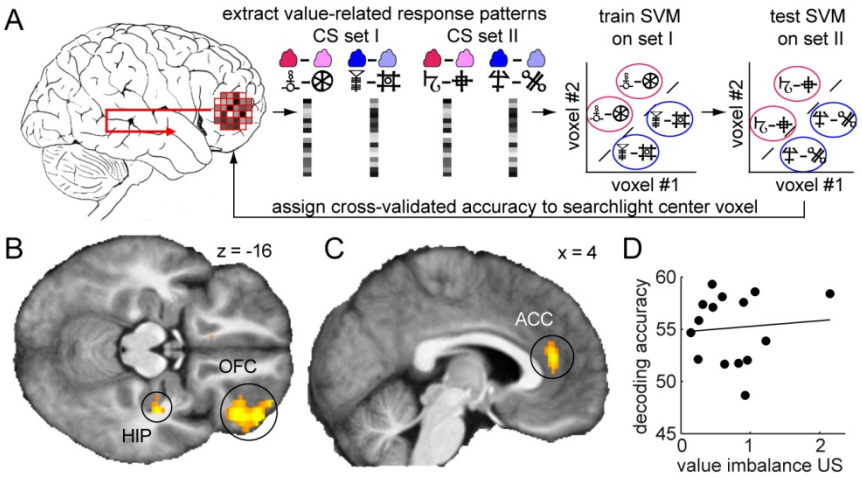


**Figure 3.** Orbitofrontal Cortex Represents Identity-Specific Predictive Values. (**A**) Schematic of the searchlight decoding analysis used to reveal identity-specific value codes. Value-related voxel responses (i.e., fMRI signal difference between high and low value conditions) were extracted for CS images predicting sweet odors (pink/red colors) and savory odors (blue colors). An SVM was trained to classify value-related response patterns for one set of CS, and then tested on the second set of CS (to ensure that effects were not driven by mere visual features of the CS images). (**B-C**) Identity-specific value responses were identified in OFC, hippocampus (HIP), and anterior cingulate cortex (ACC). Display threshold, $p < 0.001$. (**D**) Value imbalances between sweet and savory odors have no impact on identity-specific coding ($r = 0.08$, $p = 0.76$).

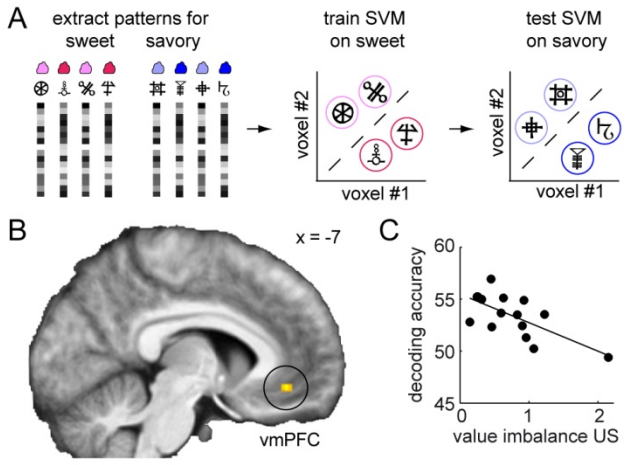


**Figure 4.** Ventromedial Prefrontal Cortex Represents Identity-General Predictive Values. (**A**) Schematic of the searchlight decoding analysis used to identify identity-independent value coding. SVM models were trained on activity patterns evoked by the CS images predicting the high vs. low value sweet odor, and then tested on patterns evoked by the CS predicting the high vs. low value savory odor (and vice versa). (**B**) Identity-general value in the vmPFC. Display threshold, $p < 0.001$. (**C**) Identity-general coding is higher when the imbalance between sweet and savory values is lower ($r = -0.68$, $p = 0.01$).

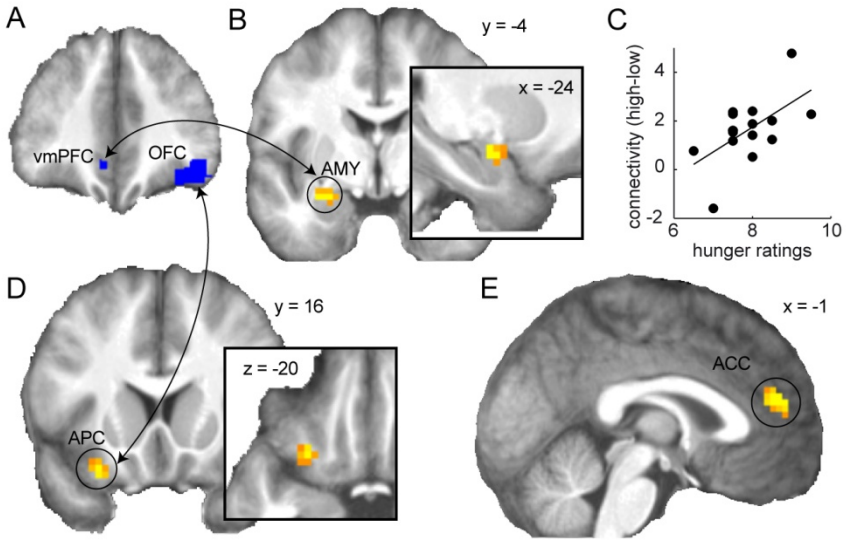


**Figure 5.** Functional Networks of General and Identity-Specific Value Coding. (**A**) Seed regions used in the functional connectivity analyses. (**B**) Voxels in the amygdala (AMY) show a general value-dependent change in connectivity with vmPFC. (**C**) Individual differences in hunger significantly predict value-related connectivity between vmPFC and amygdala ($r = 0.58$, $P = 0.02$). (**D-E**) Regions in the anterior piriform cortex (APC) (**D**) and ACC (**E**) show identity-specific value-dependent connectivity with OFC. Display threshold, $p < 0.001$.

## Supplemental Information

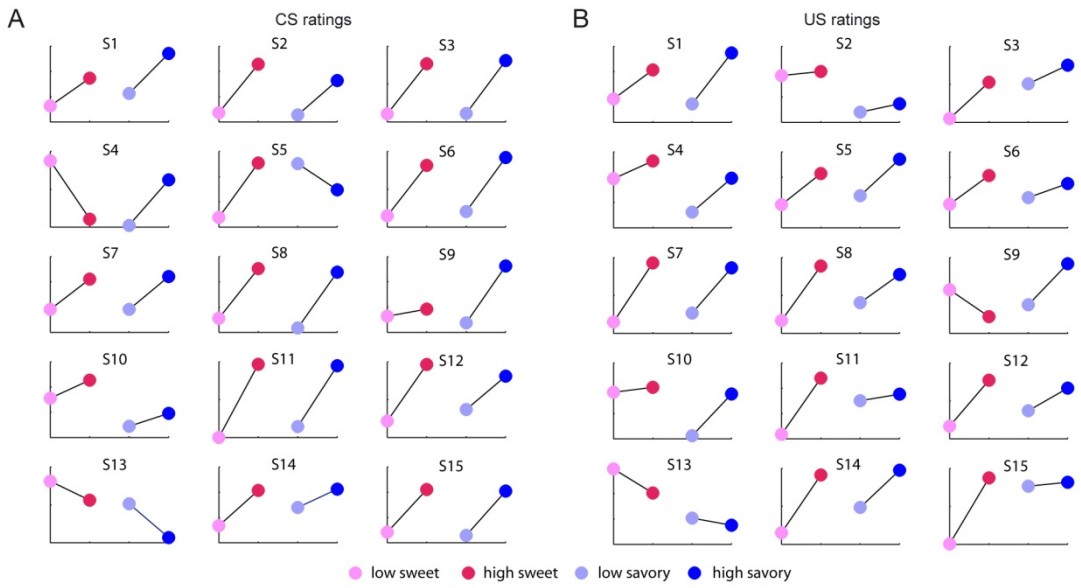


**Figure S1**. Individual pleasantness ratings. (**A**) Individual pleasantness ratings of the odor-predictive visual CS. The y-axis represents pleasantness ratings for the four odors. (**B**) Individual pleasantness ratings of the odor US. For most subjects, pleasantness is well matched between odors, but there is also some variability that could potentially confound our imaging results. We quantify this variability using the value imbalance score and include it in all statistical models. Moreover, all tests for potential confounds arising from this imbalance were not significant.

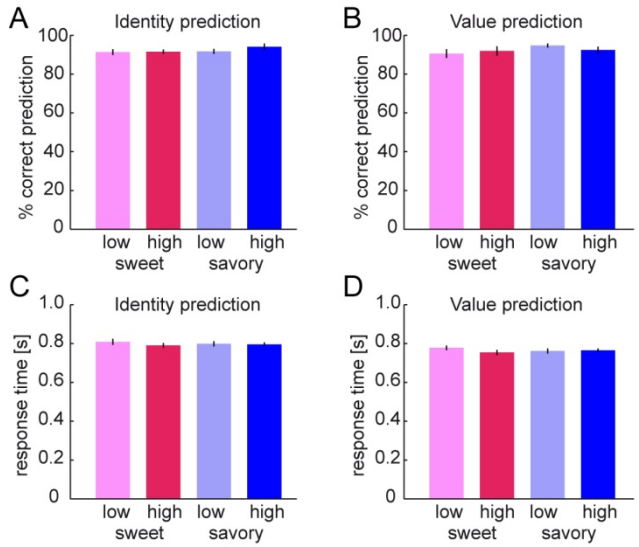


**Figure S2**. Behavioral performance and response time during the fMRI task. (**A** + **B**) During the fMRI task, subjects predicted the identity or the value (randomized across trials) of the upcoming odor outcome with high accuracy. Performance accuracy (% correct) for identity (**A**) and value predictions (**B**) did not differ (three-way [rating type by identity by value] ANOVA with repeated measures; main effect of rating type, $n = 15$; $F_{1,14} = 0.02$, p = 0.88), and accuracy did not differ as a function of predicted odor identity (main effect of identity, $F_{1,14} = 1.87$, p = 0.19) or value (main effect of value, $F_{1,14} = 0.22$, p = 0.65). None of the 2- or 3-way interactions was significant (all $Fs < 2.52$, all p's > 0.13). (**C** + **D**) Response times for identity (**C**) and value (**D**) predictions did not differ (three-way [rating type by identity by value] ANOVA with repeated measures; main effect of rating type, $n = 15$; $F_{1,14} = 4.12$, p = 0.06), and were not modulated by predicted odor identity (main effect of identity, $F_{1,14} = 0.08$, p = 0.78), or value (main effect of value, $F_{1,14} = 4.01$, p = 0.07). None of the 2- or 3-way interactions was significant (all $Fs < 1.75$, all p's > 0.20). Error bars, SEM. ($n = 15$).

## SI Materials and Methods

***Stimulus selection.*** On the first testing day, subjects provided pleasantness ratings for each of the eight odors on a labeled hedonic scale (47). For each subject, we then selected one sweet and one savory odor that were matched in pleasantness, and asked the subjects to name the odor (all subjects came up with specific sweet and savory food items) and to provide a 2 letter abbreviation for it (e.g., SB for strawberry and PZ for pizza). These names and abbreviations were used throughout the rest of the experiment. Next, we acquired pleasantness ratings for the two selected odors across a range of intensities (diluted to varying degrees with odorless air as described above). Based on these ratings, we selected two intensity levels for each odor such that the two low intensity odors had the same pleasantness and the two high intensity odors had the same pleasantness. This method is analogous to those widely used in animal studies wherein the amount of a food or liquid reward is varied to manipulate its value (2, 11, 12, 48), and takes advantage of the previously established correspondence between odor intensity and perceived odor value (18). We thus individually tailored a stimulus set for each subject consisting of four unique odors that varied independently in value and identity (**Fig. 1C**).

Pleasantness ratings of the odors and the cues on the two scanning days confirmed that they were well controlled in terms of group averages (**Fig. 2A** and **2B**). However, the decoding analyses performed here are sensitive to relative value differences within-subject (for example, if the high vs. low value difference for the *savory odor* was different from the high vs. low value difference for the *sweet odor*). Such differences could bias the classification results. In particular, relative value differences between the high and low value levels of the two odors may result in *less accurate* decoding of *identity-general* values, because these differences would decrease the sensitivity to identify common value

coding patterns. On the other hand, the same differences may spuriously induce *more accurate* decoding of *identity-specific* values because differences in value coding between the two odors would further drive classification performance over and above the effects of identity-specific value.

To estimate the subject-wise difference in relative value between the two odor identities, we computed a value imbalance score (*vi*) for the pleasantness ratings of the odors and the cues:

$$vi = \left| \left( V_{sa,h} - V_{sa,l} \right) - \left( V_{sw,h} - V_{sw,l} \right) \right|,$$

where $V_{sa,h}$, $V_{sw,h}$, $V_{sa,l}$, and $V_{sw,l}$ represent the pleasantness ratings for the high savory, high sweet, low savory, and low sweet odor (or the corresponding cues). In order to remove differences in scale usage, pleasantness ratings were z-normalized across all ratings (within-subject) before computing the index. Thus, this measure quantifies relative value differences between the two odor identities (vi = 0 indicates perfect match). The score was computed for the CS and US ratings acquired on the two scanning days, and was used as a covariate in all fMRI group level analyses.

***Classical conditioning.*** After stimulus selection on day one, we randomly assigned two different visual CS to each of the four food odors. Specifically, we used two sets of CS (set I and set II) (20) such that each odor was predicted by two CS (**Fig. 1D**). Subjects learned these associations using a classical conditioning session in which the visual CS (1500 ms) was followed directly by a sniff cue (“sniff”) and the corresponding food odor US (3000 ms). Each CS-US pairing was presented for 5 consecutive trials, followed by 7 presentation of each pairing in pseudo-random order (total of 8 x 12 = 96 trials). Trials

were separated by an interval of 10 seconds. Subsequently, subjects performed a practice version of the outcome-prediction task described below.

***Outcome-prediction task.*** On the second and third day of the experiment, subjects performed an outcome-prediction task in the scanner. On each trial, subjects were presented with one of the eight visual CS (4 odor US x 2 CS sets) for 1500 ms (**Fig. 1E**). After a variable delay of 4000-8000 ms, subjects were prompted to predict either the value (high vs. low), or the identity of the upcoming odor by making a button response with the index or middle finger of their right hand (maximal response time 1500 ms). If the response options were the letters “H” (high) and “L” (low), subjects had to predict the value; if response options were the abbreviated odor names, subjects had to predict the identity of the upcoming odor US. If the letters “XX” were presented, subjects had to withhold a response. This condition was included to dissociate anticipatory signals related to outcomes and responses. Moreover, to avoid preparatory confounds during the CS period, the type of response (value, identity, or withhold) and the position of the response options (e.g., high value prediction requiring left or right button press) were randomized on each trial. After the response was made, both response options were illuminated and stayed on the screen for the rest of the 1500 ms response window. Subjects then saw a sniff cue (“sniff”), and the corresponding odor was delivered to the subject’s nose for 3000 ms. Trials were separated by a variable interval of 4000-8000 ms. The visual CS deterministically predicted the odor US (cue-outcome contingency 100%), and each of the eight CS-US pairings was presented 4 times per run, resulting in a total of 32 trials per run in pseudo-random order.

***fMRI data acquisition.*** On each of the two scanning days, subjects performed 6 runs of the outcome-prediction task inside the MR scanner, resulting in a total of 12 scanning runs

per subject. MRI data were acquired on a Siemens 3T-scanner equipped with a 32-channel head coil. Functional imaging parameters were as follows: TR, 1510 ms; TE, 20 ms; slice thickness, 2 mm; gap, 1 mm; matrix size, 128 × 120 voxels; field of view, 220 × 206 mm. The scanning sequence was optimized for signal recovery in the orbitofrontal cortex (49) and image acquisition was tilted 30° from the horizontal axis to reduce susceptibility artifacts. In each run 385 volumes (24 slices) covering the orbitofrontal cortex, and the anterior part of the medial temporal lobe were acquired. In addition, ten whole-brain EPIs with the same imaging parameters described above (but 48 slices) were acquired for co-registration. A 1-mm isotropic T1-weighted MPRAGE structural scan was obtained, during which subjects rated the pleasantness of the odor US and the visual CS. During the experiment, sniffing was monitored using respiratory effort bands placed around the chest and abdomen. The trial-by-trial parameters for sniff amplitude and duration were computed offline and included as nuisance regressors in all fMRI analyses.

***fMRI pre-processing.*** Pre-processing of the functional imaging data was performed using SPM8 (Wellcome Department of Imaging Neuroscience, Institute of Neurology, London, UK), and included slice-time correction and re-alignment to the first volume. Whole brain EPIs were re-aligned and the mean EPI was co-registered (rigid-body) to the mean re-aligned functional EPI. The co-registered whole-brain EPI was then normalized to the MNI template in order to estimate normalization parameters, which were then applied to the accuracy maps from the decoding analysis.

**SI Discussion**

Our study utilizes the quantity of odor molecules in the air (hereafter intensity) as a way to manipulate the pleasantness of the odor (hereafter value). In other words, intensity is the value-relevant physical stimulus dimension in our study. This is in line with the well-established link between intensity and pleasantness (17), and with previous studies that used intensity to manipulate reward value (18). Importantly, this manipulation is structurally equivalent to changing the amount of a liquid (1, 2, 13, 50-57) or solid food reward (8, 48, 58) to manipulate value, as has been done in many animal studies of reward processing, learning and decision-making. Just as in our current experiment, in the studies cited above, quantity is the value-relevant dimension that is manipulated in order to change the reward value of the reinforcer.

In theory, our results could therefore be explained by expected intensity, rather than expected value. However, there is a solid body of evidence suggesting that the observed effects are unlikely to be driven by expected intensity as opposed to value. First, BOLD signals in the OFC do not change with value-matched changes in odor intensity (59, 60). Second, BOLD signals in the OFC are sensitive to intensity-matched changes in odor value (59) or with devaluation-induced changes in expected and experienced odor value (16, 61).

Nevertheless, to provide empirical evidence that our findings are not related to levels of odor intensity, we tested whether across-subject decoding accuracies in OFC are correlated with differences in expected odor intensity. Specifically, as was done with our measure of value imbalance, we computed the difference in intensity between high and low intensity odors, and compared this difference between the two odors. If decoding

accuracy were based on general predicted odor intensity, differences in intensity between the two odors would degrade decoding accuracy for identity-general value. That is, we would expect a negative correlation between identity-general value coding and intensity imbalance. In contrast, decoding accuracy for identity-specific value would be enhanced (positively correlated) with this measure of intensity imbalance. However, this analysis revealed that neither of these correlations was significant (general value, $r = -0.15$, $p = 0.58$; identity-specific value, $r = -0.12$, $p = 0.66$), suggesting that decoding accuracy was not based on expected intensity.

On a related note, it is unclear whether it is possible at all to manipulate the value of a reward independent of its identity. In other words, intensity/quantity/magnitude could be just another sensory feature of the expected outcome that is represented by OFC activity. In this framework, reward value is not a separable feature of what is expected but rather the sum of all sensory features of the expected outcome that constitute its value-relevant meaning to the organism.

Notably, identity-specific value signals were not only found in the OFC but also in the ACC and hippocampus, along with significant functional connections between OFC and ACC. Even though value coding neurons are found throughout both regions (34, 62), functional specialization exists for value processing in ACC and OFC. Specifically, compared to OFC, responses in ACC have been shown to primarily reflect action-reward associations (62, 63) and value during foraging decisions (64, 65). However, recent empirical and computational studies suggest that ACC does not signal signed value, but rather unsigned signals such as choice difficulty (66), unsigned associative value (i.e., salience) (20), or unsigned prediction errors (i.e., surprise) (67, 68). Although we are unable to distinguish

between these alternative explanations, our findings suggest that value-related signals in ACC – whether signed or unsigned – are specific to the identity of the expected outcome.

In contrast to ACC and OFC, the hippocampus is typically engaged in value-based behavior in the context of higher-order associations (69, 70) and generalization (71, 72). These functions involve processing the similarities, differences, and other relations amongst stimuli, highlighting the importance of the hippocampus in processing stimulus identity. We speculate that the hippocampus is involved in retaining sensory-based information about specific rewards which may be linked to value-based representations in OFC for later consolidation. This idea is in line with anatomical connections linking the hippocampus to the OFC (39) and, via the entorhinal cortex, to primary olfactory cortices (31).